ELSEVIER

Chemical Engineering Journal 133 (2007) 229–237

Chemical Engineering Journal

www.elsevier.com/locate/cej

Carbon dioxide absorption into monoethanolamine in a continuous film contactor

Akanksha [a], K.K. Pant [a,*], V.K. Srivastava [b]

[a] *Department of Chemical Engineering, Indian Institute of Technology, Delhi, Hauz Khas, New Delhi 110016, India*
[b] *Dean, Academic Affairs, ABES College, Ghaziabad, India*

Received 10 September 2006; received in revised form 13 December 2006; accepted 1 February 2007

Abstract

Numerical approach for analyzing absorption rate and understanding of the micro level interactions of various processes going inside the reactor was proposed by developing a mathematical model. The usefulness of this approach is demonstrated by presenting the analysis of experimental data for CO_2 absorption into aqueous solutions of monoethanolamine. A continuous film contactor has been designed and developed for carrying out the absorption studies experimentally. The model equations were solved using computer code in conjunction with a non-linear regression technique to estimate a correlation, first of its kind, for physical gas-phase mass transfer coefficient. Proposed numerical scheme simulates the results based on momentum, mass and heat balance at the gas–liquid interface to explain the absorption behaviour. Results showed a good agreement between experimental and model predictions, thereby suggesting the utility of the model in predicting the chemical gas-absorption performance of gas liquid contactors.

Keywords: Absorption; Film contactor; Modeling; CO_2; Monoethanolamine

1. Introduction

Gas absorption using liquid absorbents is one of the common mass-transfer operations widely used in industries for separating gases that are useful, toxic or environmentally unfavourable species. Separating carbon dioxide (CO_2) from flue gases exhausted by fossil-fuel-fired power plants, pharmaceutical industry, petroleum industry, etc., a potential measure to mitigate the human-originated greenhouse effect, requires the use of a gas–liquid contact device that efficiently removes CO_2 from a flue-gas flow at an enormously high rate without imposing on the flow such a substantial pressure loss as to necessitate the addition of a flue-gas compression process. Thus for treating huge amount of low-pressure (not much higher than atmospheric pressure) gases of no further use, it is critically important to devise gas–liquid contactors that allow effective gas absorption without pressurizing the gases to balance the hydrodynamic pressure losses inside the contactors. Packed columns have been widely used in industries for separation and purification processes involving gas and liquid contact (such as distillation and absorption) due to its high efficiency and high capacity but are not well suited for processing huge amounts of industrial waste gases due to inevitable insufficient contact-area-to-volume ratios and large gas-side pressure losses during operation. Thus from all the available designs, continuous film contactors for processing flue gases or other industrial waste gases are considered to be more advantageous. These are vertical columns where liquid flows downward wetting the wall while the gas flow counter currently contacting the liquid.

Various technologies have been developed for CO_2 and H_2S removal from gas streams. These include absorption by chemical and physical solvents, cryogenic separation and membrane separation. Gas absorption by chemical solvents such as aqueous solution of alkanolamine is one of the most popular and effective methods compared to other methods. Absorption of gas using alkanolamines has been practiced in industry for over half a century; however, it is only recently that substantial progress has been made in developing a fundamental understanding of these seemingly simple processes. A number of mathematical models for falling film reactors have been proposed [1–8] in the field of absorption, however limited attempts have been to include

* Corresponding author. Tel.: +91 11 26596172; fax: +91 11 26581120.
E-mail address: kkpant@chemical.iitd.ac.in (K.K. Pant).

1385-8947/$ – see front matter © 2007 Elsevier B.V. All rights reserved.
doi:10.1016/j.cej.2007.02.001

Nomenclature

a_c	correction factor for the interfacial area, $R_w(d - 2\delta)/d$
A	gaseous reactant
b	stoichiometric coefficient of B
B	liquid reactant
c	concentration of reactant gas (kg/m^3)
C_A	concentration of dissolved gas A (kmol/m^3)
C_{AG}	concentration of A in bulk gas (kmol/m^3)
C_B	concentration of reactant B (kmol/m^3)
C_B^o	inlet concentration of reactant B (kmol/m^3)
c_G	molar heat capacity of gas (J/kmol K)
$c_p\rho$	heat capacity of liquid (J/m^3 K)
d	inner diameter of the column (m)
D_A	diffusivity of A in liquid (m^2/s)
D_B	diffusivity of B in liquid (m^2/s)
D_G	diffusion coefficient of CO_2 in gas (m^2/s)
f	friction coefficient
F	dimensionless group containing flow rates and fluid properties defined in Eq. (15)
g	acceleration of gravity (m/s^2)
h_G	heat transfer coefficient in gas phase (J/s m^2 K)
H_o	Henry's constant (kmol/m^3)$_{gas}$/(kmol/m^3)$_{liquid}$
$-\Delta H_R$	heat of reaction (J/kmol)
$-\Delta H_S$	heat of solution (J/kmol)
k	second order rate constant at a temperature T_r (m^3/kmol s)
k_G	mass transfer coefficient (m/s)
k_λ	thermal conductivity of liquid (J/s m K)
L	height of the column (m)
Q_G	volumetric flow rate of gas (m^3/s)
r	rate of reaction (kmol/m^3 s)
R	gas constant (J/kmol K)
R_A	rate of gas absorption (kg/s)
Re_G	gas-phase Reynolds number, $(d - 2\delta)u_G\rho_G/\mu_G$
Re_L	liquid-phase Reynolds number, $4\Gamma/\mu_L$
R_W	ratio of the interfacial area in the presence of waves to the plane interfacial area
Sc_G	Schmidt number, $\mu_G/\rho_G D_G$
Sh_G	Sherwood number, $k_G a_c d/D_G$
T	liquid temperature (K)
T_G	gas-phase temperature (K)
T_o	inlet liquid temperature (K)
T_R	temperature of cooling water (K)
u_L	axial velocity of liquid film (m/s)
u_G	velocity of gas film (m/s)
U	overall heat transfer coefficient for cooling water (J/s m^2 K)
w_G	molar flow rate of gas per unit wetted perimeter (kmol/(m s))
x	radial coordinate (m)
z	axial coordinate (m)

Greek letters

α	thermal diffusivity (m^2/s)
β	function of liquid film Reynolds number, defined in Eq. (16)
Γ	volumetric liquid flow rate (m^3/s)
δ	liquid film thickness (m)
μ	liquid viscosity (kg/m s)
ν	kinematic viscosity of liquid (m^2/s)
ρ	liquid density (kg/m^3)
τ	shear stress (N/m^2)

Subscripts

G	gas phase
i	interface
in	inlet
L	liquid phase
out	outlet

realistic fluid mechanics to model the liquid film flow. Several researchers [9–18] have illustrated the mass transfer studies, in particular, for the chemical absorption of CO_2 into aqueous solutions of amines like monoethanolamine (MEA), diethanolamine (DEA) and methyl-diethanol amine (MDEA) and its mixtures. Among them, the use of aqueous MEA solutions as absorbent takes more share in the industrial processes of CO_2 removal and research concerned have been reported [14–16]. Recently, sterically hindered amines such as 2-amine-2-methyl-1-propanol (AMP) have also found commercial application in gas treating industries.

The present work is to develop a mathematical model that can predict the non-isothermal absorption using observational knowledge of configurations and motion of the film. An empirical correlation for the dimensionless mass transfer coefficients, (Sh_G) in falling film reactor at low Reynolds numbers is determined based on the experimental investigations, which was used directly in the modeling equations. Experimental results were utilized in estimating gas-absorption performance in a continuous film contactor.

2. CO_2 absorption experiments

2.1. Apparatus and procedure

The schematic diagram of the experimental setup is shown in Fig. 1. The setup consists of three major sections: (1) the main part of the unit or the reactor section consisting of jacketed tubular falling liquid film column, (2) the liquid flow section consisting of the trough and peristaltic pump and (3) gas collection section consisting of gas sampler and a gas-chromatograph for identifying the gaseous components.

The reactor was made of glass (inner diameter 0.014 m, length 1 m) and cooling water was circulated through the jacket. The liquid was fed by peristaltic pump into the trough (holding capacity ~0.12 mL) of the liquid flow section from where it was made

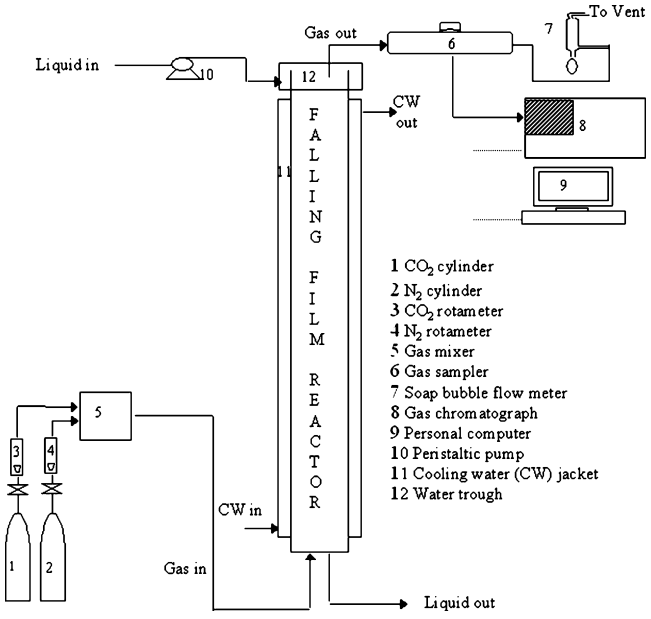

Fig. 1. Experimental setup.

to flow downward wetting the walls of the reactor. Feed gas (a mixture of CO_2 and N_2) was introduced from the bottom of the reactor and flows upward in the main reaction section counter current to the liquid phase.

All the experiments were conducted at 298 K temperature and 1 atm pressure. CO_2 gas was diluted to the desired concentration with nitrogen before entering the reactor. The absorbent (30% aqueous MEA) selectively absorbs the CO_2 gas from the feed gas mixture and reacts simultaneously to form a stable carbamate in the reactor section. The gas samples were analysed using a gas chromatograph with Chromosorb 104 packed column in conjunction with a Model WinAcds 6.2 (Aimil Ltd.). The inlet and outlet gas-phase composition was determined using thermal conductivity detector with helium used as carrier gas (flow rate of 25 cm^3/min). Oven, injector and detector temperatures were kept at 363 K, 383 K and 373 K respectively. Knowing the inlet and exit gas (CO_2) composition, the mass rate of absorption was calculated.

The properties of the absorbent i.e., 30 wt.% aqueous MEA solution, and of the CO_2–absorbent system are summarized in Table 1. The gas and liquid flow rates used were 1.67×10^{-5} to 5.0×10^{-5} m^3/s and 1.04×10^{-7} to 4.72×10^{-7} m^3/s respectively. The higher velocity of the MEA solution was determined so as to maximize the flow while the lower one was set close to the lower border of the stable film flow.

2.2. Results and discussion

For evaluating the effectiveness of CO_2 transfer, rate of absorption (mass based), R_A defined as

$$R_A = Q_G c_{out} - Q_G c_{in} \quad (1)$$

was used, where c denotes the mass of CO_2 transferred from a unit volume of the gaseous mixture, and subscripts "in" and "out" indicate the gas mixture sampled before and after the liquid

Table 1
Physical and chemical properties of CO_2-MEA system, temperature 298 K and a total pressure of 101.32 kPa

Absorbent	30 wt.% MEA solution
Density, ρ_L (kg/m^3)	1010
Viscosity, μ_L (kg/m s)	2.41×10^{-3}
Thermal conductivity, k_λ (W/m K)	0.4837
Surface tension (N/m)	55.1×10^{-3}
Liquid diffusivity of CO_2, D_A (m^2/s)	1.42×10^{-9}
MEA diffusivity D_B (m^2/s)	1.10×10^{-9}
Diffusivity of CO_2 in gas, D_G (m^2/s)	1.67×10^{-5}
Density of gas mixture, ρ_G (kg/m^3)	1.248
Viscosity of gas mixture, μ_G (kg/m s)	1.72×10^{-5}
Henry constant, H_o (kmol/m^3 kPa)	0.316×10^{-3}
Heat of reaction (kJ/kmol)	65,000
Heat of solution (kJ/kmol)	19,500

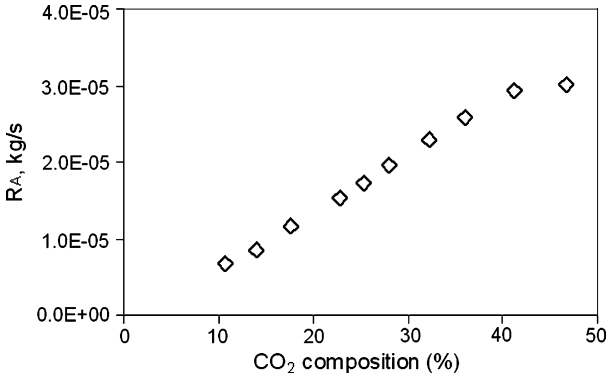

Fig. 2. Effect of CO_2 concentration on rate of absorption, $u_G = 0.3236$ m/s, $u_L = 0.0412$ m/s, MEA concentration = 30 wt.%.

flowing down the test column. The effect of operating parameters on CO_2 absorption was studied by conducting series of experiments by varying CO_2 partial pressure, amine concentration and gas–liquid flow rates. It was observed that with increase in CO_2 partial pressure, the rate of absorption increases (Fig. 2). This is because; higher CO_2 mole fraction enhances the rate of interfacial transfer by lowering the gas side mass transfer resistance. The increase in gas velocity also exhibited similar behaviour on the rate of absorption (Fig. 3). This contributes to enhanced rate of mass transfer associated with the higher gas Reynolds number due to the interfacial turbulence caused by large ampli-

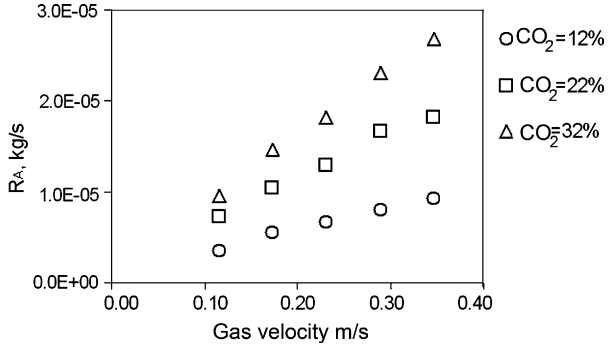

Fig. 3. Effect of gas velocity on rate of absorption for different CO_2 concentrations, $u_L = 0.0412$ m/s, MEA concentration = 30 wt.%.

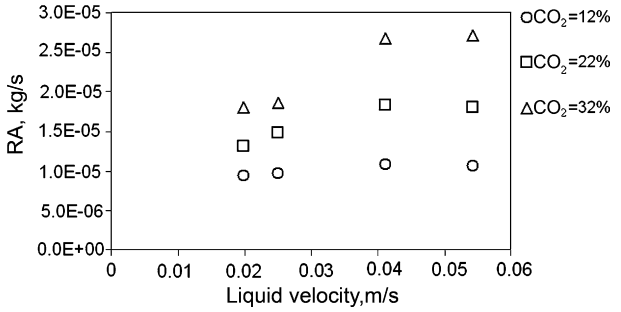

Fig. 4. Effect of liquid velocity on rate of absorption for different CO_2 concentrations, $u_G = 0.3467$ m/s, MEA concentration = 30 wt.%.

tude waves. The effect of changing liquid flow was studied and found that higher liquid flow rate presumably increases the rate of absorption (Fig. 4). This effect is surmised to occur due to the increase in film thickness, which leads to larger concentration gradient thereby increasing R_A. The rate of absorption was found to increase with the increase in MEA concentration (Fig. 5). Use of higher liquid composition results in more reaction due to more film thickness. Moreover, the higher viscosity may cause the liquid to flow down the reactor more slowly, yielding a longer residence time in the test column for a fixed liquid velocity.

2.3. Mass transfer correlation

A differential mass balance over the gas phase for the absorbed component results in the following equation for mass transfer coefficient (k_G):

$$k_G = \frac{Q_G}{\pi(d-2\delta)R_w L} \ln\left(\frac{C_{AGin}}{C_{AGout}}\right) \quad (2)$$

where R_w is the ratio of the interfacial area in the presence of waves to the plane interfacial area. Its value is equal to 1 for plane liquid films and is >1 for wavy films of very high flow rates. Since the liquid film is not plane, a correction factor, a_c, is to be introduced and defined as [19],

$$a_c = \left(\frac{d-2\delta}{d}\right) R_w \quad (3)$$

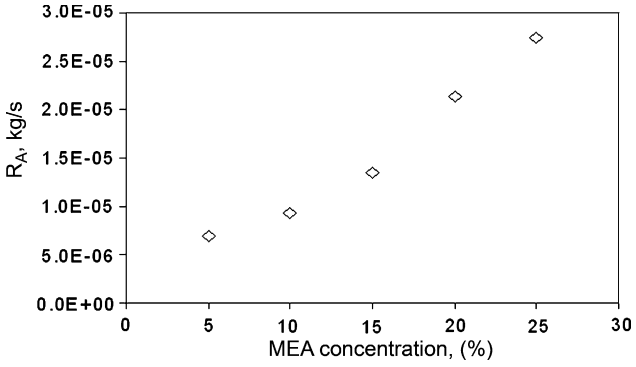

Fig. 5. Effect of MEA composition on rate of absorption for $u_G = 0.3467$ m/s, $u_L = 0.0412$m/s, CO_2 concentration = 30 mol%.

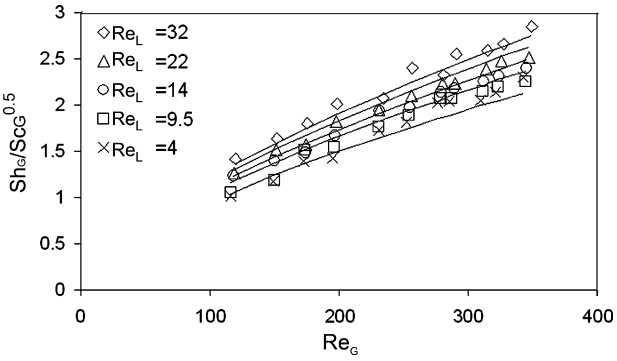

Fig. 6. Experimental gas-phase mass transfer coefficient data (symbols) compared with fitted correlation, Eq. (5) (solid line).

Eq. (2) is rewritten by the use of Eq. (3) and the following corresponding expression is obtained:

$$\frac{Q_G}{\pi d} \ln\left(\frac{C_{AGin}}{C_{AGout}}\right) = k_G a_c L \quad (4)$$

All the uncertainities concerning the interfacial area are lumped into the final data and expressed as $k_G a_c$.

The modified gas-phase mass transfer coefficient, $k_G a_c$, was calculated from Eq. (4) at different gas and liquid flow rates. The other terms of the equations were determined experimentally. Experimental data and the fitted correlation, given by Eq. (5), were compared in Fig. 6, in which $Sh_G/Sc_G^{0.5}$ is plotted against Re_G for five different values of Re_L. All these dimensionless numbers are defined in nomenclature. The correlation is based on 55 data points and predicts the experimental data with a mean deviation of 3.9%

$$Sh_G = 0.0387 Re_G^{0.66} Re_L^{0.115} Sc_G^{0.5} \quad (5)$$

The coefficients of Eq. (5) are estimated using non-linear least-square regression by fitting the expression to the experimental data. The correlation is valid for $Re_G \in [115; 350]$ and $Re_L \in [4; 32]$ at 298 K. The dependency of Re_L is probably due to changes in the interfacial area and increased turbulence of the fluid phases. It was not possible to find any suitable correlations in the literature for comparison with Eq. (5) because earlier investigations were conducted at higher Reynolds number.

3. Modeling of chemical gas-absorption

A numerical model has been developed for predicting the rate of absorption of any species initially mixed in a gas phase by a chemically reactive liquid flowing down a reactor wall. It has been modified according to the CO_2-MEA system with CO_2 as gas species and MEA as liquid for better comparison and for validating with the experimental results described in the preceding section.

3.1. Basic assumptions

The basic assumptions considered for the CO_2 absorption by MEA solution in a falling film flow are listed below:

1. The physical properties of the liquid are held constant over the entire gas–liquid contact section irrespective of the special variation in the concentration of the liquid due to its absorption of CO_2.
2. The film thickness is small compared to the column diameter.
3. The liquid film is symmetric with respect to the reactor axis.
4. The CO_2 solubility in the liquid reactant and in the reaction products is in accordance with the Henry's law.
5. The liquid reactant is assumed to be non-volatile at working temperatures.

Assumption (1) is surmised to be reasonably accurate because the axial change in liquid composition in the gas–liquid contact section is expected to be insignificant. It should be noted that since the film thickness is very small compared to the column radius, and since the flow is symmetric in vertical annular flow, the flow is formulated as two-dimensional, and a Cartesian coordinate system is used instead of cylindrical coordinates, thus simplifying the model.

3.2. Formulation

3.2.1. CO_2-MEA reaction

The overall reaction occurring in the liquid phase may be expressed as

$$CO_2 + 2RNH_2 \rightarrow RNH_3^+ + RNHCOO^- \quad (6)$$

where R indicates $HCOH_2CH_2$. This overall reaction is second order, i.e., first order with respect to CO_2 and MEA separately [20], and thus the reaction rate r, being defined as the molar rate of loss of CO_2 per unit volume, is expressed in terms of a reaction rate constant k and molar concentrations of CO_2 and MEA, C_A and C_B, as follows:

$$r = kC_AC_B \quad (7)$$

where k can be calculated, using the empirical correlation given by Hikita et al. [20].

3.2.2. Model equations

The modeling includes all the three transfer processes i.e., mass, momentum and heat to study the coupled effect of temperature and concentration on the rate of absorption. The developed equations include both ordinary differential equations (ODE's) and partial differential equations (PDE's) of non-linear nature. The flow model is described in Fig. 7.

The coupled partial differential equations representing the mass and heat balances for reaction

$$A(G) + bB(L) \rightarrow \text{Product} \quad (8)$$

can be written as follows.

3.2.2.1. Liquid phase.

(i) Momentum balance

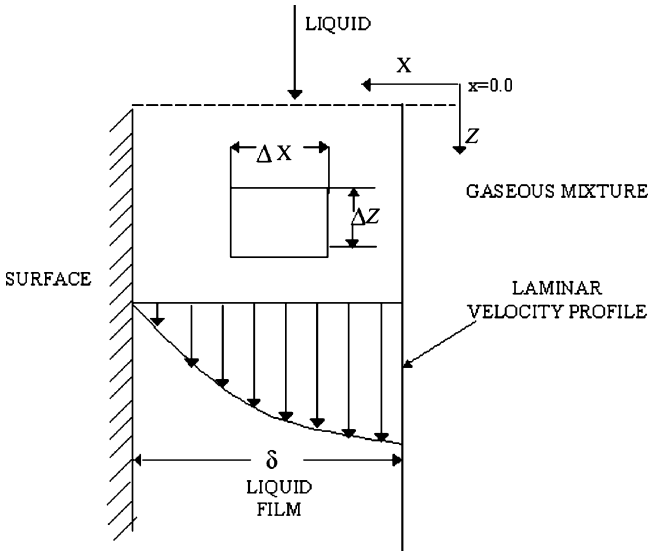

Fig. 7. Flow model of the film reactor.

The governing differential equation describing the momentum balance is given as:

$$\frac{d\tau_{xz}}{dx} = \rho g \quad (9)$$

Applying the following boundary conditions gives velocity distribution as given by Eq. (11), where

- Boundary conditions

$$\text{At } x = 0, \text{ interface, } \tau_{xz} = \tau_i = -\tau_G,$$
$$\text{At } x = \delta, \text{ wall, } u_L = 0 \quad (10)$$

- Velocity distribution

$$u_L = \frac{\rho_L g}{2\mu_L}\delta^2\left[1 - \left(\frac{x}{\delta}\right)^2\right] - \frac{\tau_G\delta}{\mu_L}\left[1 - \left(\frac{x}{\delta}\right)\right] \quad (11)$$

Film thickness, δ is calculated from the volumetric rate of liquid obtained by the integration of the velocity distribution (Eq. (11)) and is given as

$$\Gamma = \frac{\rho g}{3\mu}\delta^3 - \frac{\tau_G\delta^2}{2\mu} \quad (12)$$

where

$$\tau_G = f\rho_G u_G^2 \quad (13)$$

The friction factor, f was evaluated using the relations proposed by Henstock and Hanratty [21], which accounts for the irregularities at the surface of the liquid layer and is given by

$$\frac{f}{2} = \begin{cases} \dfrac{8}{Re_G} & Re_G < 2000 \\ \dfrac{Re_G^{0.33}}{3050} & 2000 < Re_G < 4000 \\ \dfrac{0.04}{Re_G^{0.25}} & Re_G > 4000 \end{cases} \quad (14)$$

To account for the two-phase flow nature, the friction factor for $Re_G > 4000$ given by Eq. (14) should be multiplied by a term $(1 + 1400F)$ where for the laminar liquid film,

$$F = \frac{\beta(Re_L)}{Re_G{}^{0.9}} \frac{\nu_L}{\nu_G} \frac{\rho_L}{\rho_G} \left[1 - \exp\left(-\frac{\tau_G}{\rho_L g \delta}\right)\right] \quad (15)$$

in which

$$\beta = [(0.707 Re_L^{1/2})^{2.5} + (0.0379 Re_L^{0.9})^{2.5}]^{0.4} \quad (16)$$

(ii) Mass balance

- For component A:

$$u_L \frac{\partial C_A}{\partial z} = \frac{\partial}{\partial x}\left[D_A \frac{\partial C_A}{\partial x}\right] - kC_A C_B \quad (17)$$

- For component B:

$$u_L \frac{\partial C_B}{\partial z} = \frac{\partial}{\partial x}\left[D_B \frac{\partial C_B}{\partial x}\right] - kbC_A C_B \quad (18)$$

(iii) Heat balance

$$u_L \frac{\partial T}{\partial z} = \frac{\partial}{\partial x}\left[\alpha \frac{\partial T}{\partial x}\right] + \left(\frac{\Delta H_R}{\rho c_p}\right) kC_A C_B \quad (19)$$

- Boundary equations:

For $x = \delta$ at the wall

$$\frac{\partial C_A}{\partial x} = 0, \qquad \frac{\partial C_B}{\partial x} = 0,$$

$$-k_\lambda \frac{\partial T}{\partial x} = U(T_{x=0} - T_R) \quad (20)$$

For $x = 0$ at the interface

$$k_G(C_{AG} - C_A H_o) = -D_A \frac{\partial C_A}{\partial x}, \qquad \frac{\partial C_B}{\partial x} = 0,$$

$$h_G(T - T_G) - k_\lambda \frac{\partial T}{\partial x} = (-\Delta H_s)\left[D_A \frac{\partial C_A}{\partial x}\right] \quad (21)$$

At $z = 0$,

$$C_A = 0, \qquad C_B = C_B^o, \qquad T = T_o \quad (22)$$

3.2.2.2. Gas phase.

(i) Mass balance

$$\frac{d w_G C_{AG}}{dz} = k_G(C_{AG} - H_o C_A) \quad (23)$$

(ii) Heat balance

$$\frac{d(w_G c_G T_G)}{dz} = h_G(T_{x=0} - T_G) \quad (24)$$

3.3. Numerical solution procedure

The mathematical relations were incorporated into an iterative solution procedure to elucidate the rate of CO_2 absorption changes with respect to the fall distance of the MEA solution. The algorithm for the numerical model is given in Appendix A. The complexity of the model can be seen from the counter current flow direction of the two phases resulting into two iterative loops, whereas all the mathematical models reported in the past [1–8] are for co-current flow thus simplifying the numerical procedure. These coupled PDE's were solved using backward implicit finite difference numerical scheme. Implicit trapezoidal scheme was used to solve the gas-phase heat and mass transport equations. The tridiagonal matrix obtained from the discretization of highly coupled partial differential equation was solved using a subroutine wherein the $M \times M$ matrix was modified into $M \times 3$ matrix thereby reducing the computer storage space and processing speed [22].

By specifying the experimental conditions and physical properties of the MEA solution and of the CO_2/MEA binary system, $C_{AG}(z)$ was computed and subsequently R_A, the rate of absorption defined by Eq. (1) in which c_{in} and c_{out} should be read as $C_{AG,z=L}$ and $C_{AG,z=0}$ respectively. The results thus obtained are exemplified in Figs. 8–11 together with corresponding experimental results. The goodness of fit between

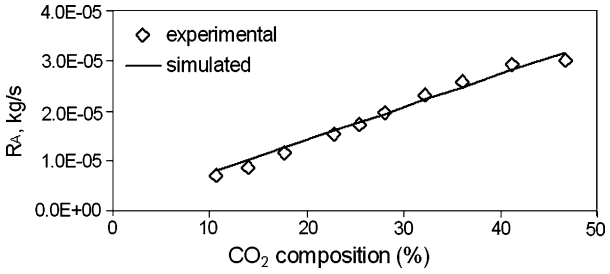

Fig. 8. Comparison of predicted R_A with corresponding experimental data (effect of changing CO_2 concentration).

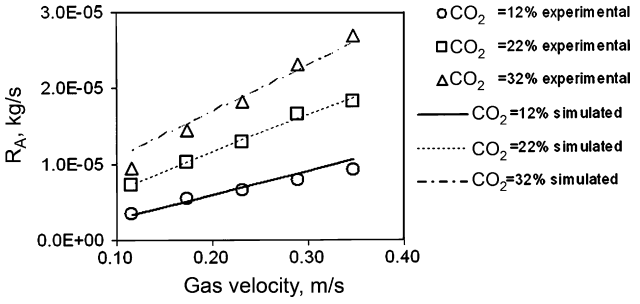

Fig. 9. Comparison of predicted R_A with corresponding experimental data (effect of changing gas flow rate).

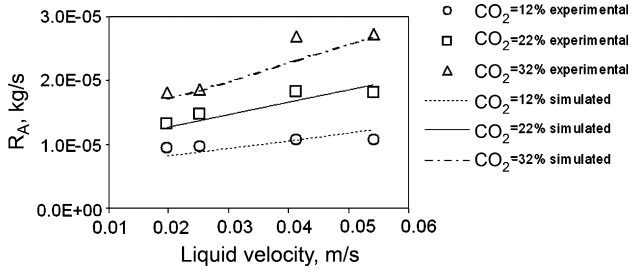

Fig. 10. Comparison of predicted R_A with corresponding experimental data (effect of changing liquid flow rate).

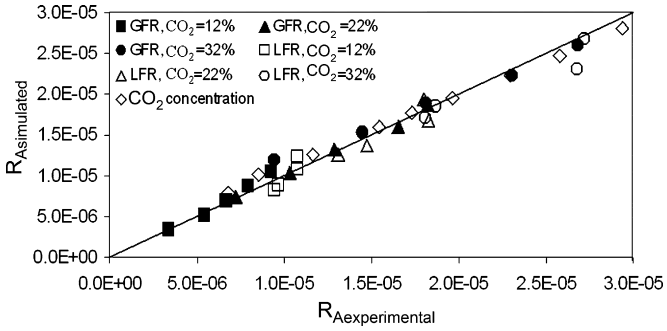

Fig. 11. Parity plot of experimental and predicted values.

predicted and experimental data indicates the practical utility of the chemical absorption model described above in predicting actual gas-absorption performance of a falling film reactor.

4. Conclusion

CO_2 absorption by MEA in a continuous film contactor has been experimentally analyzed and found better than other conventional processes. The proposed numerical scheme simulating the results based on momentum, mass and heat balance provides a mechanistic interpretation of the experimental results, and a means to predict the gas-absorption performance at arbitrary adjustments of operational parameters such as reactants (gas and liquid) concentration, flow rate of the absorbent, and flow rate of the gas mixture. The gas-phase mass transfer coefficient was also measured for laminar range of gas and liquid-phase Reynolds numbers. Reasonably good agreement between the model predictions and corresponding experimental results supports the general validity of the physical view underlying the model. The effect of gas and liquid temperature on the rate of absorption will be the next phase of this study.

Appendix A. Algorithm for the numerical model

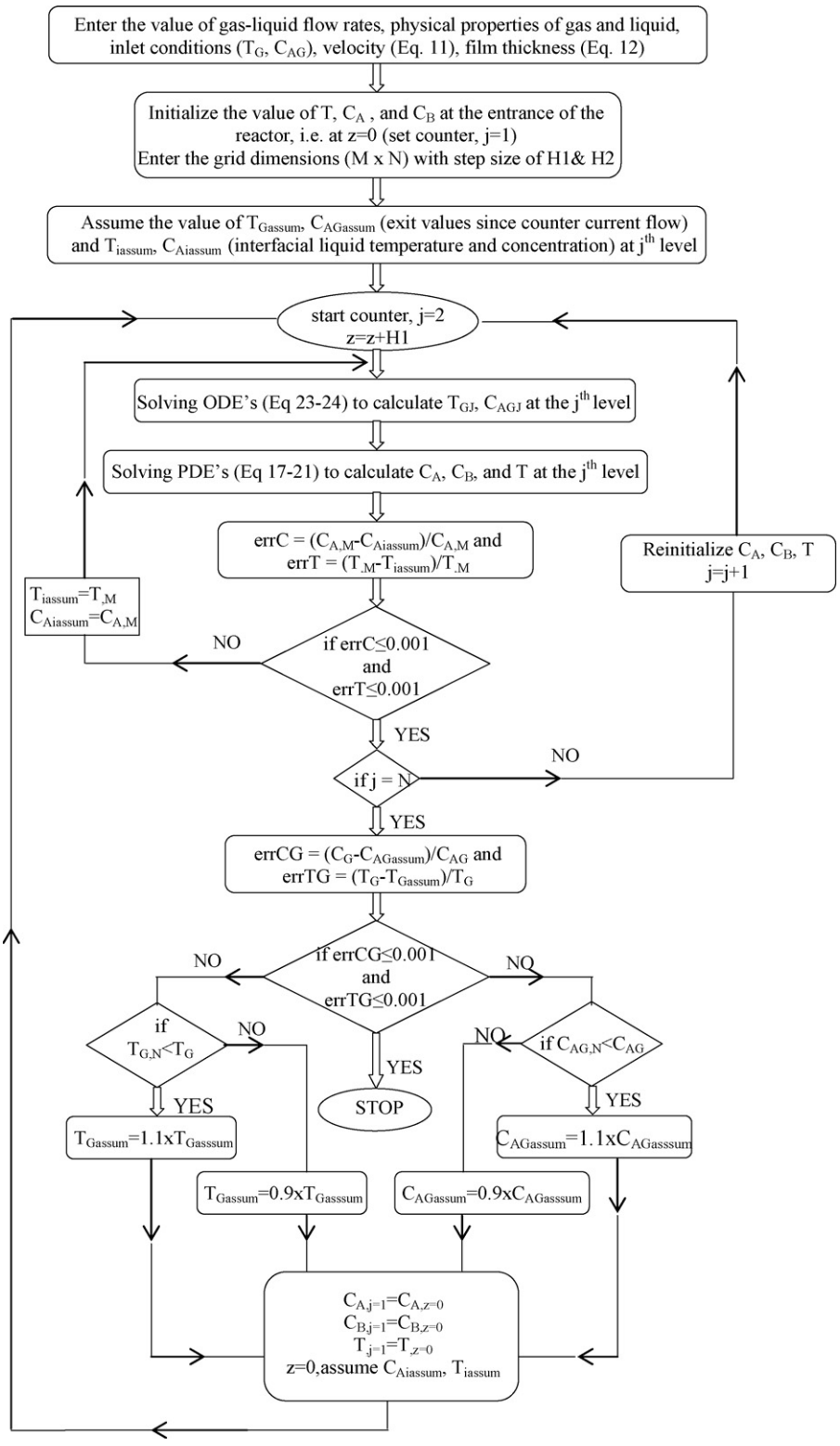

References

[1] G.R. Johnson, B.L. Crynes, Modeling of a thin film sulphur trioxide sulphonation reactor, Ind. Eng. Chem. Process Des. Dev. 13 (1974) 6–14.

[2] E.J. Davis, M.V. Ouwerkerk, S. Venkatesh, An analysis of the falling film gas–liquid reactor, Chem. Eng. Sci. 34 (4) (1979) 539–550.

[3] R. Mann, H. Moyes, Exothermic gas absorption with chemical reaction, AIChE J. 23 (1) (1977) 17–23.

[4] J. Gutierrez, C. Mans, J. Costa, Improved mathematical model for a falling film sulphonation reactor, Ind. Eng. Chem. Res. 27 (1988) 1701–1707.

[5] B. Dabir, M.R. Riazi, H.R. Davoudirad, Modelling of falling film reactors, Chem. Eng. Sci. 51 (11) (1996) 2553–2558.

[6] A. Bhattacharya, R.V. Gholap, R.V. Chaudhari, Gas absorption with exothermic bimolecular reaction in a thin liquid film: fast reactions, Can. J. Chem. Eng. 66 (1988) 599–604.

[7] P.H. Nielsen, J. Villadsen, Absorption with exothermic reaction in a falling film column, Chem. Eng. Sci. 38 (9) (1983) 1439–1454.

[8] P.H. Nielsen, J. Villadsen, An analysis of the multiplicity pattern of models for simultaneous diffusion, chemical reaction and absorption, Chem. Eng. Sci. 40 (4) (1985) 571–587.

[9] B.P. Mandal, M. Guha, A.K. Biswas, S.S. Bandyopadhyay, Removal of carbon dioxide by absorption in mixed amines: modelling of absorption in aqueous MDEA/MEA and AMP/MEA solutions, Chem. Eng. Sci. 56 (21–22) (2001) 6217–6224.

[10] P.M.M. Blauwhoff, G.F. Versteeg, W.P.M. Van Swaaij, A study on the reaction between CO_2 and alkanolamines in aqueous solutions, Chem. Eng. Sci. 38 (9) (1983) 1411–1429.

[11] H. Bosch, G.F. Versteeg, W.P.M. Van Swaaij, Gas–liquid mass transfer with parallel reversible reactions. I. Absorption of CO_2 into solutions of sterically hindered amines, Chem. Eng. Sci. 44 (11) (1989) 2723–2734.

[12] H. Bosch, G.F. Versteeg, W.P.M. Van Swaaij, Gas–liquid mass transfer with parallel reversible reactions. II. Absorption of CO_2 into solutions of sterically hindered amines, Chem. Eng. Sci. 44 (11) (1989) 2735–2743.

[13] G.F. Versteeg, J.A.M. Kuipers, F.P.H. Van Beckum, W.P.M. Van Swaaij, Mass transfer with complex reversible chemical reactions. II. Parallel reversible chemical reactions, Chem. Eng. Sci. 45 (1) (1990) 183–197.

[14] K. Uchiyama, H. Migita, R. Ohmura, Y.H. Mori, Gas absorption into "string-of-beads" liquid flow with chemical reaction: application to carbon dioxide separation, Int. J. Heat Mass Transfer 46 (3) (2003) 457–468.

[15] H. Migita, K. Soga, Y.H. Mori, Gas absorption in a wetted-wire column, AIChE J. 51 (8) (2005) 2190–2198.

[16] K.A. Hoff, H.F. Svendsen, O. Juliussen, O.F. Pedersen, M.S. Gronvold, D.B. Stuksrud, The Kvaerner/Gore membrane process for CO_2 removal mathematical model and experimental verification, in: AIChE Annual Meeting, Los Angeles, 2000.

[17] A. Jamal, A. Meisen, C.J. Lim, Kinetics of carbon dioxide absorption and desorption in aqueous alkanolamine solutions using a novel hemispherical contactor. I. Experimental apparatus and mathematical modelling, Chem. Eng. Sci. 61 (19) (2006) 6571–6589.

[18] A. Jamal, A. Meisen, C.J. Lim, Kinetics of carbon dioxide absorption and desorption in aqueous alkanolamine solutions using a novel hemispherical contactor. II. Experimental results and parameter estimation, Chem. Eng. Sci. 61 (19) (2006) 6590–6603.

[19] C.H.E. Nielsen, S. Kiil, H.W. Thomsen, K.D. Johansen, Mass transfer in wetted-wall columns: correlations at high Reynolds numbers, Chem. Eng. Sci. 53 (3) (1998) 495–503.

[20] H. Hikita, S. Asai, Y. Katsu, S. Ikuno, Absorption of carbon dioxide into aqueous monoethanolamine solutions, AIChE J. 25 (5) (1979) 793–800.

[21] W.H. Henstock, T.J. Hanratty, The interfacial drag and the height of the wall layer in annular flows, AIChE J. 22 (6) (1976) 990–1000.

[22] V.K. Srivastava, The thermal cracking of benzene in a pipe reactor, Ph.D. Thesis, University of Wales, Swansea, UK, 1983.